

# Transport properties of Ti–Ni spinel ferrites

M.R. Eraky<sup>a,\*</sup>, S.M. Attia<sup>a,b</sup>

<sup>a</sup> Physics Department, Faculty of Science, Kafrelsheikh University, 33516 El Geesh Street, Kafr El-Sheikh, Egypt

<sup>b</sup> Physics Department, College of Applied Sciences, Umm Al-Qura University, PB 7296, Makkah 21955, Saudi Arabia



## ARTICLE INFO

### Article history:

Received 3 August 2014

Received in revised form

8 November 2014

Accepted 14 January 2015

Available online 15 January 2015

### Keywords:

Semiconductors

Electrical transport

Ferrites

NiTi ferrite.

## ABSTRACT

Polycrystalline ferrites with the composition  $Ti_xNi_{(1-x)}Fe_{(2-2x)}O_4$  ( $0 \leq x \leq 0.625$ ) were prepared by a double sintering ceramic method. Results of DC electrical resistivity,  $\rho_{DC}$ , versus a temperature ensured that the samples possess a semiconductive character. Results of Seebeck coefficient  $S$  reveal that pure Ni ferrite is n-type semiconductor while the sample with  $x=0.625$  is p-type semiconductor over the whole range of temperature. However, for other samples,  $S$  shows a transition from p-type to n-type semiconductor with increasing temperature. On the basis of  $\rho_{DC}$ ,  $S$  and  $\rho_{AC}$ , the conduction mechanism of Ni–Ti ferrite was determined.

© 2015 Elsevier B.V. All rights reserved.

## 1. Introduction

Owing to their magnetic character, ferrites play an important role in a wide field of technological applications. Spinel ferrites are commercially important materials due to their interesting electric and magnetic properties [1,2]. Tailoring of a material with specific properties such as magnetic, electric, electromagnetic and thermal properties depend mainly on the method of preparation, types and amount of doping and the conditions of sintering (such as sintering time, temperature and surrounded atmosphere). Among spinel ferrites, pure nickel ferrite  $NiFe_2O_4$ , is particularly important during the last few decades. Studies of Ni–ferrites with different metal ions such as Cu, Zn, Cd, Li, Co and Mg have been carried out by many workers [3–8]. Kale et al. studied the crystal structure and Mössbauer spectra for  $Ti^{4+}$  substituted nickel ferrite and established a detailed map for cation distribution in  $Ti_xNi_{(1-x)}Fe_{(2-2x)}O_4$  ferrite [9]. Hall effect and thermoelectric power data are usually needed for the interpretation of the conduction mechanism in semiconductors. However, in the case of low mobility semiconductors such as ferrite, it is sometime difficult to measure the Hall effect. Alternatively, the thermo emf measurements become an easy and effective method for determining the type of charge carrier and its concentration in ferrite. In the present work we gradually replace both divalent ions ( $Ni^{2+}$ ) and matrix ions ( $Fe^{3+}$ ) in Ni–ferrite with  $Ti^{4+}$  to improve and modify the electrical and thermal properties of nickel ferrite. In this paper, the results of DC, AC and thermoelectric power were used to study

the electrical and thermal properties for  $Ti_xNi_{(1-x)}Fe_{(2-2x)}O_4$  ( $0 \leq x \leq 0.625$ ).

## 2. Material and methods

Polycrystalline samples of  $Ti_xNi_{(1-x)}Fe_{(2-2x)}O_4$  (where  $x=0.0, 0.125, 0.25, 0.375, 0.50, \text{ and } 0.625$ ) are prepared by a double sintering ceramic method. A mixture of highly purified and dried  $NiO$ ,  $TiO_2$  and  $Fe_2O_3$  was grinded for 4 h using the electric grinding machine. The pre-sintering of the final mixture was achieved at  $1050^\circ\text{C}$  for 6 h and re-grinded for 10 h. The obtained fine powders compressed into pellets using a hydraulic press under 70 bar for 2–3 min, and then sintered at  $1200^\circ\text{C}$  for 6 h in air. The heating process of the samples started at room temperature up to  $600^\circ\text{C}$  at rate  $6^\circ\text{C}/\text{min}$  and then kept at  $3^\circ\text{C}/\text{min}$  to the final sintering temperature. The cooling rate was  $2^\circ\text{C}/\text{min}$  from sintering temperature to  $600^\circ\text{C}$  and then the furnace was turned off. The bulk density of the samples,  $D_B$ , was determined from the relation:

$$D_B = m/\pi r^2 t \quad (1)$$

where  $m$  is the mass,  $r$  is the radius and  $t$  is the thickness of the sample. X-ray density,  $D_X$ , was calculated using the following formula [10]:

$$D_X = 8M/N_A a^3 \quad (2)$$

where  $M$  is the molecular weight of the sample,  $N_A$  is Avogadro's number and  $a$  is the lattice parameter. The porosity,  $P$ , was calculated by the relation [11]:

\* Corresponding author. Fax: +20 473215175,  
E-mail address: [moharamderak@yahoo.com](mailto:moharamderak@yahoo.com) (M.R. Eraky).

$$P = ((D_x - D_B)/D_x) \times 100\% \quad (3)$$

The disks with thickness  $\sim 3$  mm and diameters  $\sim 13$  mm were polished to obtain smooth parallel surfaces.

The crystal structure was characterized by X-ray diffraction carried out using SHIMADZU XRD6000 diffractometer with Cu K $\alpha$  radiation ( $\lambda = 1.54060$  Å) at a speed of  $8^\circ/\text{min}$  and step of  $0.02^\circ$ .

For measurements of thermoelectric power,  $S$ , the samples were placed between two nonmagnetic copper electrodes in a silica tube cell, which surrounded at the middle by a heating coil to vary the temperature inside the tube. An auxiliary small heating coil was wound around one of the two electrodes to achieve a temperature difference of  $\Delta T$  ( $\Delta T = T_2 - T_1 \approx 10$  °C) between the two surfaces of the sample. The temperatures of the two surfaces ( $T_1, T_2$ ) were measured using k-type thermocouples. The thermovoltage ( $\Delta V$ ) was measured using digital nanovoltmeter (Keithley 175 nanovoltmeter). The sign of the thermovoltage was determined from the polarity of the cold end of the sample since the charge carriers migrate from hot to cold end. The thermoelectric power was determined by the value  $\Delta V/\Delta T$ .

DC electrical resistance was measured by the two probe method on the basis of Ohm's law. The resistance of the sample was determined directly by a digital electrometer (type 617 Keithley). Details about the experimental technique were given in our previous work [12].

AC electrical resistivity  $\rho_{AC}$ , was determined by two probe method using an LCR meter (Model HIOKI 3532-50 LCR Hi tester). AC resistivity was measured in the frequency range 100 Hz–5 MHz at room temperature.

This work was carried out at the Physics Department, Faculty of Science, Kafrelsheikh University, Kafr El-Sheikh, Egypt.

### 3. Results and discussion

#### 3.1. Composition and XRD

X-ray diffraction patterns of  $\text{Ti}_x\text{Ni}_{(1-x)}\text{Fe}_{(2-2x)}\text{O}_4$  ( $0 \leq x \leq 0.625$ ) are shown in Fig. 1. The diffraction peaks were indexed and all these peaks belong to spinel cubic structure only. The lattice parameter of Ni–Ti spinel ferrite system was determined from  $d$ -spacing according to the following equation [10]:

$$a = d \sqrt{h^2 + k^2 + l^2} \quad (4)$$

where,  $a$  = lattice parameter,  $d$  = inter planar distance and ( $h, k, l$ ) are Miller indices. The calculated lattice parameters and the diffraction peaks identify a single phase of a cubic spinel crystal structure for these samples.

Fig. 2 shows the variation of the lattice parameter,  $a$ , with Ti content  $x$ . It is shown that the lattice parameter increases with increase of Ni and Ti ion substitution. The value of the lattice parameter for  $\text{NiFe}_2\text{O}_4$  ( $x=0.0$ ) is 0.837 nm, which found to be in a good agreement with that reported by K. R. Krishna et al. [13]. The variation of lattice constant with substitution indicates that the substitutions were achieved on crystallographic sites. The mean ionic radius of the variant ions,  $r_{(\text{variant})}$ , for the  $\text{Ti}_x\text{Ni}_{(1-x)}\text{Fe}_{(2-2x)}\text{O}_4$  composition can be written as follows:

$$r_{(\text{variant})} = x r_{\text{Ti}} + (1-x) r_{\text{Ni}} + (-2x) r_{\text{Fe}}$$

where  $r_{\text{Ti}}$  is the ionic radii of  $\text{Ti}^{4+}$  ions ( $=0.068$  nm [14]),  $r_{\text{Ni}}$  is the ionic radii of  $\text{Ni}^{2+}$  ions ( $=0.078$  nm [14]), and  $r_{\text{Fe}}$  is the ionic radii of  $\text{Fe}^{3+}$  ions ( $=0.064$  nm [14]). The variation of  $r_{(\text{variant})}$  increases with increasing both Ti and Ni ion content instead of Fe ion (Fig. 2).

The values of X-ray density,  $D_x$ , bulk density,  $D_B$ , molecular

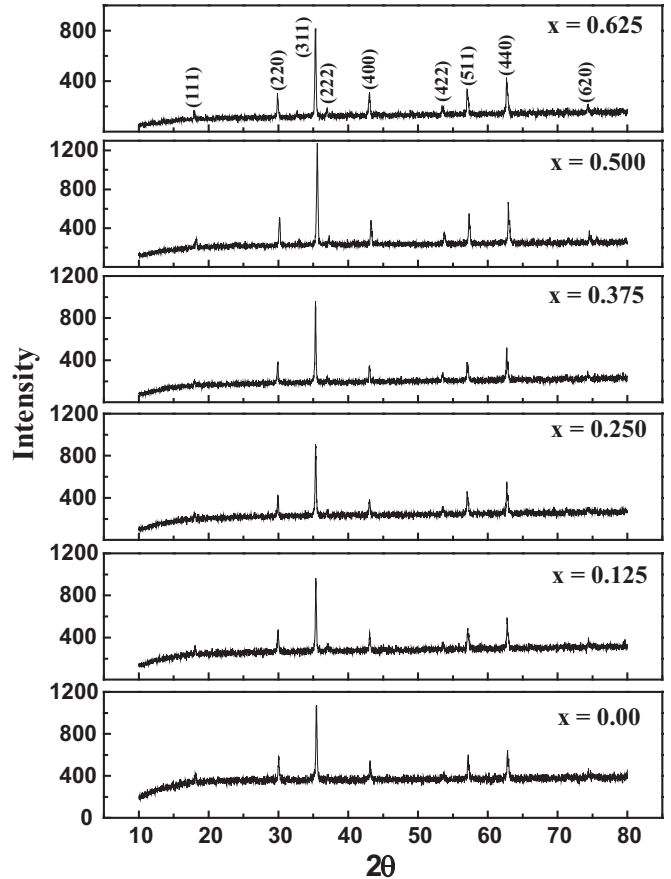


Fig. 1. : X-ray diffraction patterns for  $\text{Ni}_{(1-x)}\text{Ti}_x\text{Fe}_{(2-2x)}\text{O}_4$  spinel ferrites.

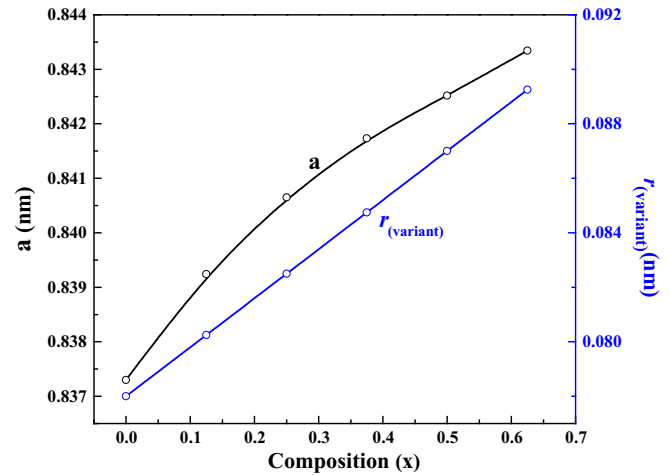


Fig. 2. : Variation of lattice parameter,  $a$ , and the radius of the variant,  $r_{(\text{variant})}$ , with  $x$  for  $\text{Ni}_{(1-x)}\text{Ti}_x\text{Fe}_{(2-2x)}\text{O}_4$  spinel ferrites.

weight, MW, cell volume,  $V$ , and porosity,  $P$ , for Ni–Ti ferrite are listed in Table 1. It is shown that X-ray density,  $D_x$  decreases with increasing  $x$ . This behavior can be explained on the basis of the decrease of molecular weight of the composition and the increase of the unit cell volume with increasing  $x$ . On the other hand, X-ray density is higher than the bulk density due to the existence of pores. The values of the porosity are inversely proportional to the values of bulk density (Table 1), indicating that dense ferrites have less pores.

Download English Version:

<https://daneshyari.com/en/article/1809111>

Download Persian Version:

<https://daneshyari.com/article/1809111>

[Daneshyari.com](https://daneshyari.com)